JOURNAL OF CATALYSIS 28, 245-253 (1973)

Microfocused X-ray Diffraction Examination of Pt/Al_2O_3 Catalysts Before and After Engine Dynamometer Aging

K. MIYAZAKI

Mitsui Mining and Smelling Company, Central Research Laboratories,
Mitaka, Tokyo, Japan

Received April 26, 1972

Microstructural changes in the surface crystallinity of supported platinum with time in aging were examined by means of microfocused X-ray diffraction technique. Two typical commercially available platinum catalysts in pellet form, 0.5% Pt-Al_2O_3, were served for automotive exhaust oxidation under nonleaded engine dynamometer driving condition. It was revealed that the platinum-dispersed alumina layer on the support, extending approximately 100-200 μm deep from the surface, possessed a disordered crystalline arrangement distinguishable from the usual form of platinum and from the internal alumina matrix. The initial adherent form of platinum with rather well crystalline character exhibited a higher activity of CO and HC (hydrocarbons) oxidation, than the one with amorphous form of platinum. It has been shown that deactivation of catalyst under nonleaded condition is closely associated with alteration in crystalline orientation of this characteristic thin zone of the catalyst surface.

INTRODUCTION

There are many complex causes of deactivation of working catalysts in commercial processes (*1*). However, it is generally recognized that these causes would fall into two categories, one, chemical, and the other physical, factors. In the case of catalysts tried for automotive exhaust conversion application, deactivation phenomena with time in use can also be considered from these two aspects.

As a representative chemical factor, lead severely decreases the activity of platinum catalyst (*2, 3*). An example of the chemically attacked surface of a supported platinum pellet exposed to leaded automotive exhaust is illustrated in Fig. 1, which was readily examined by means of electron probe microanalysis (*4*). The line profiles scanned in the arrowed directions across the radially sectioned catalyst tablets indicated that the surface zone was strongly contaminated with lead after use (Fig. 1f). The lead occupied the platinum layer as well as diffused in the subsurface of alumina supports to the depth of approximately 100–130 μm.

In other words, from a chemical point of view, microstructural change can be evidently visualized by use of a microanalytical tool as being one of the poisoning factors relating loss in activity of catalyst.

Another factor to be taken into account for is definitely the effect of physical factors. With a catalyst of base metal oxides, such as manganese–copper oxides, silver oxide–barium peroxide, and copper-promoted iron oxide, the result of inspection on the bulk of the material by powder X-ray diffraction method was reported in a previous paper (*5*) that the catalyst would undergo phase changes during use at an elevated temperature.

However, to date, there seems to be very little information available regarding the phase change which might take place in the surface zone itself, apart from the averaged one observable with the entire body of catalyst pellets. This is especially true when one discusses deactivation of a sup-

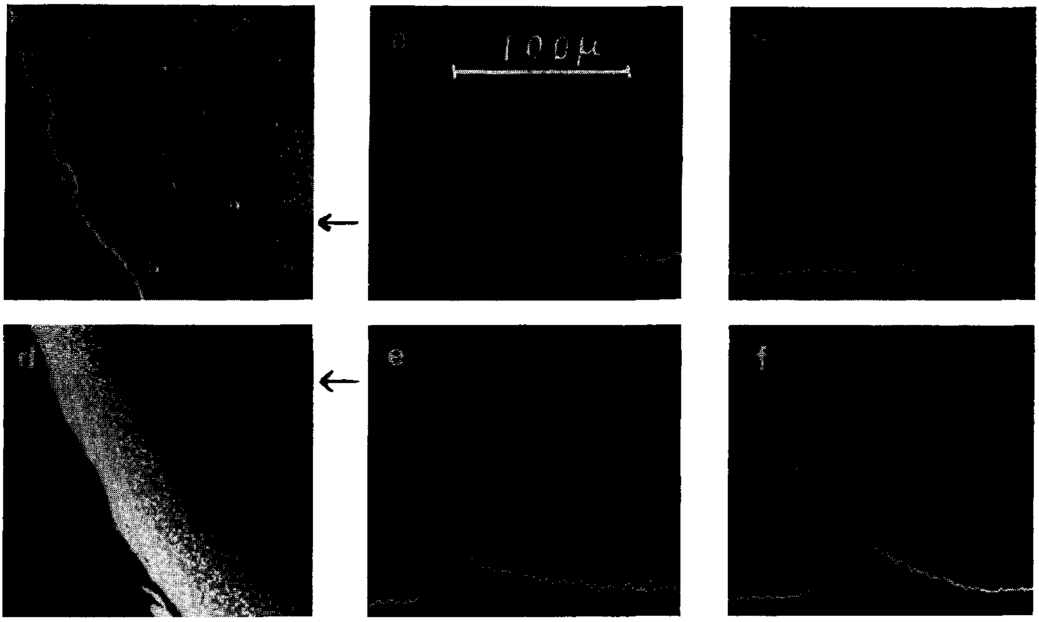

FIG. 1. Electron probe microanalysis of radial cross-sections of a Pt–Al_2O_3 catalyst before and after use in leaded automotive exhaust. (I, top row), before use; (II, bottom row), after use; (a), backscattered electron image; (b), and (c), line profiles of $K\alpha$ rays of Pt and Pb scanned in the arrowed direction.

ported platinum under nonleaded conditions. A microstructural physical change, if any, occurring in a minor amount of the active material, usually less than 1%, might not emerge with a meaningful picture in the conventional powder X-ray diffraction chart. Platinum is generally considered to more readily withstand high temperatures than most of the base metals. However, it is also known that the noble metal catalyst does lose its activity gradually even with no lead to chemically attack the surface. A structural rearrangement is most likely to occur in the surface zone consisting of platinum layer dispersed in the alumina matrix.

Thus, when one defines the surface zone to be the platinum dispersed in alumina, extending as thin as in the order of 100 μm deep from the surface, no clear understanding has ever been established in the past as for alteration of physical microstructure in the surface zone during nonleaded automotive exhaust aging.

In recent years, a newly developed technique of a nondestructive X-ray diffraction with microfocused X-ray beam has been increasingly used in such fields as metallurgy and ceramic sciences in determining the processes of crystal recovery, recrystallization, and grain growth (*6*). The principle is that monochromatic X-rays generated from mini-sized target are collimated into a microbeam less than 200 μm in diameter and focused onto selected area of specimen under investigation (*7*).

In the present study, two typical commercially available Pt–Al_2O_3 catalysts were subjected to engine dynamometer aging with nonleaded gasoline, and have been inspected with this tool focusing the microbeam of X-rays onto thin areas of surface zone of the catalysts. The purpose here is to determine if a microstructural physical change has occurred in platinum–alumina thin zone accompanying loss in activity during the catalyst aging.

EXPERIMENTAL METHODS

Materials and Procedures

Two typical supported platinum catalysts, catalyst A and B of 0.5% Pt–Al_2O_3, respectively, which were commercially available in pellet form, were subjected to dynamometer aging. The catalysts were exposed to hot exhaust gas of a 1600 cc engine to work for oxidation of CO and HC (hydrocarbons) contained in the 420–440°C inlet under an accelerating driving condition as follows:

> Engine driving, 2000 rpm; boost, -100 mm Hg; fuel, nonleaded gasoline (94 RON); residual Pb content of the nonleaded gasoline, 0.0125 g/liter; exhaust gas composition, CO 1.9–2.2%, HC 50–100 ppm, NO_x 1400–1600 ppm, O_2 2.0–2.1%, CO_2 12.5–13.0%, balance N_2 and H_2O, added secondary air, 80–90 liter/min; space velocity, 45 000 hr^{-1}; and quantity of catalyst, 1.4 liter per batch.

The catalyst samples were removed with time at 0, 100, and 200 hr aging, and the following measurements were carried out.

(1) Specific activity of CO and HC conversions retained with the aged samples, and

(2) Microfocused X-ray diffraction examination on surface layer with radially sectioned specimens.

Apparatuses

Specific activity test. A portion of the dynamometer aged samples was transferred to a minireactor with a bed volume of 10 ml to study the decline of the specific activity due to aging. For the feedstream to the minireactor, another set of a 1600 cc engine bench was driven and the waste gas was fed together with added secondary air. This engine was constantly run under a lightload condition and the waste gas was used as a feed for general purpose activity test. Typical analysis of the inlet was as follows: 2.8–3.2% CO, 100–120 ppm HC, 4.9–5.1% O_2, 9.0–9.2% CO_2, 1–2% H_2O, and 79–82% N_2. The H_2O content of the feed to the minireactor was lower than as was exhausted in the engine manifold, since the water was partially condensed in the distributing piping on the way from the engine bench to the minireactor section. The temperature of the inlet was controlled by a preheater, and no external heating was applied to the reactor zone containing the catalyst sample. When oxidation commenced, the temperature of the bed rose above that of the inlet gas stream. Increase of inlet temperature by 50–100°C corresponded to an increase of bed temperature by more than 200°C. Therefore, readout of temperature was more conveniently done from the bed than from the inlet gas. This also avoided a possible erroneous effect due to heat radiation from the preheater to the inlet.

Comparative activity curves in terms of CO and HC conversion rates versus bed temperatures were obtained with the catalyst samples taken before and after aging. Nondispersive infrared analyzers and associated instruments were used to measure the CO and HC concentrations of inlet and outlet of the minireactor bed.

Microfocused X-ray diffraction examination of catalyst. Each aged sample was mixed with an epoxy resin and molded into a button approximately 2 cm in diameter and 1 cm thick. The button was sectioned across the pellet in order to expose the radially transversed area of the catalyst and the facet of the button was well polished. The polished specimen was mounted to a microfocused X-ray diffraction device so that the sectioned tablet was facing the X-ray microbeam source. The X-ray microbeam, collimated to approximately 100 μm in diameter, was focused onto a selected area of the transversed section corresponding to the surface zone of the original tablet. This procedure was done with an aid of optical system to permit viewing the area to be irradiated. A simple version of the instrument is shown in Fig. 2. One commercial unit was used. A typical example of optical picture showing how the X-ray microbeam is positioned onto the thin surface zone is illustrated in Fig. 3.

Due to limitation of the space provided by the device, the largest allowable size of film to be installed was 4 × 4 cm. The film was placed as close as possible to the facet of the mounted specimen producing the backscattered X-rays, leaving a space of 5 mm. Either a copper, chromium or iron target was employed to obtain the X-ray

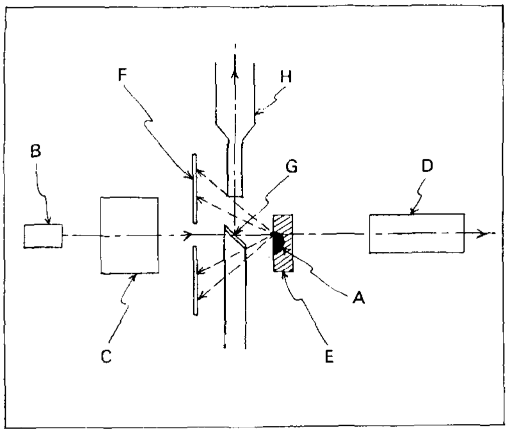

FIG. 2. Schematic diagram of microfocused X-ray diffraction reflection instrument. (A), cross-sectioned catalyst tablet; (B), X-ray source; (C), collimator; (D), detector; (E), resin mount; (F), film; (G), mirror; and (H), optical microscope.

diffraction reflection rings on the film. Under these conditions, an upper limit observable for the value of crystal lattice spacings (d) was 1.183 Å for (311) of platinum, and 1.395 Å for (440) of gamma alumina, respectively.

RESULTS AND DISCUSSION

A typical microprobe scan of the pellet used with nonleaded gasoline is shown in Fig. 4. It is illustrated with the line profiles of Pt (Fig. 4a) and of Pb (Fig. 4b) that there was no appreciable amount of lead adhered to the platinum zone on the surface which was examined after a 200-hr engine dynamometer aging.

Figure 5 shows that initially the rise of slope of curves for CO oxidation commenced at a bed temperature of 100°C with catalyst A, and around 150°C with catalyst B. Catalyst A achieved conversion rate of almost 99% for CO at a bed temperature of 350°C, and catalyst B, nearly 98% at 430°C. However, as the aging proceeded deactivation noticeably took place. The ignition temperature characterized by the rise of the curves has shifted to higher regions of temperature, around 150°C with catalyst A and to more than 220°C with catalyst B. At this stage the maximum attainable conversion rates were also shifted to higher temperature zones such as 380°C for catalyst A giving 98%, while 440°C for catalyst B giving 97%, respectively. Both catalysts were further deactivated at 200- than at 100-hr aging. Totally, however, catalyst A suffered a larger loss in activity than catalyst B. These observations are somewhat more discernible in activity measurement for HC oxidation rates shown in Fig. 6. Both catalyst samples required higher ignition temperatures, and showed much lower levels of attainable oxidation rates. The two catalysts exhibited a same type of pattern of loss

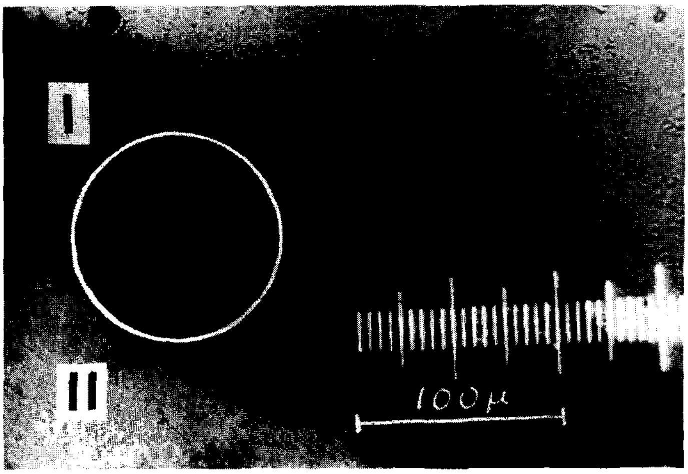

FIG. 3. Positioning of X-ray microbeam, 100 μm in diameter, onto platinum-dispersed alumina layer of a transversed catalyst tablet.

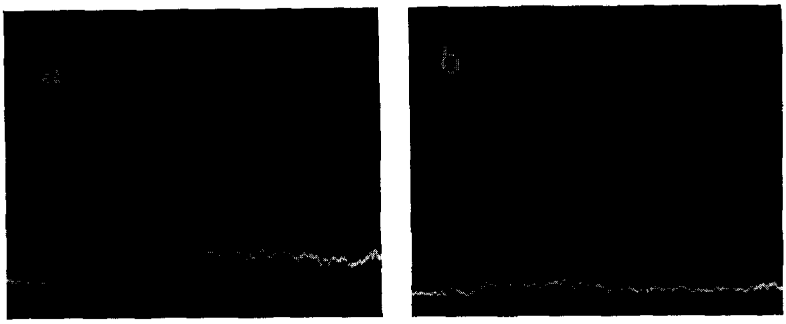

FIG. 4. Typical line profiles of Pt (a), and Pb (b) $K\alpha$ rays scanned in the diametrical direction of catalyst pellet used with nonleaded gasoline, showing that no appreciable lead is adhered to the surface zone after use.

in HC oxidation activity as seen in CO oxidation due to the aging procedure.

Many investigators pointed out for the noble metal catalysts that the activity of a freshly prepared catalyst almost invariably changes with time in use (*8*), and studies of sintering of Pt–Al_2O_3 catalysts in air reported that there was a steady decline in activity and in surface area related to the sintering time (*9*). Meanwhile, some experimental results elsewhere observed no straightforward relationship between catalyst activity and the surface area (*10*).

Table 1 shows the BET surface area measurement carried out with tablet samples of catalysts A and B before and after the aging operation. Although the initial activity of catalyst A was superior to B (see Figs. 5 and 6), no appreciable difference in surface areas was seen for initial state of the catalysts. Furthermore, the decrease in the surface area is not parallel to the extent of deactivation seen in the two catalysts. This will simply support that the surface area is not always the governing factor in this particular case, and there should be another factor to be taken into account in describing surface characteristics of a catalyst.

TABLE 1

BET SURFACE AREA OF CATALYST SAMPLES BEFORE AND AFTER AGING PROCEDURE

Samples	0 hr	100 hr	200 hr
Catalyst A	96 m^2/g	73	73
Catalyst B	95	85	85

Table 2 shows the microfocused X-ray

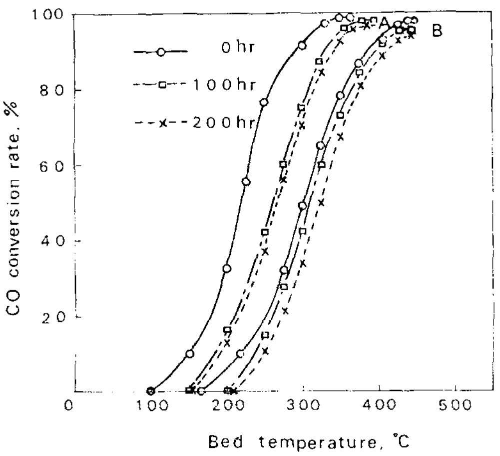

FIG. 5. Changes in CO oxidation rates versus bed temperature of catalysts A and B with aging time.

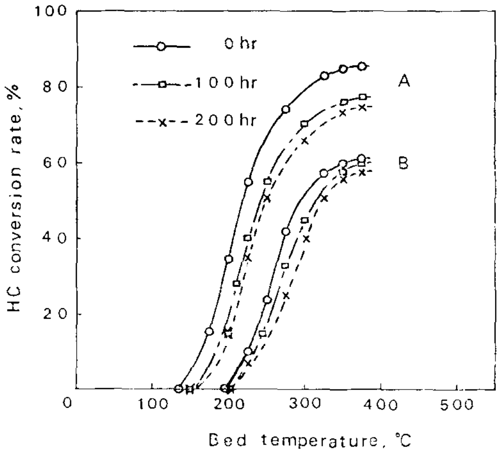

FIG. 6. Changes in HC oxidation rates versus bed temperature of catalysts A and B with aging time.

TABLE 2

Microfocused X-Ray Diffraction Reflection from Cross-Sectioned Surface Zone of Catalyst A Before Engine Dynamometer Aging

Platinum						Gamma alumina					
ASTM data			Observed data			ASTM data			Observed data		
d (Å)	I/I_0	hkl	d (Å)	I/I_0	hkl	d (Å)	I/I_0	hkl	d (Å)	I/I_0	hkl
1.387	31	(220)	Not appreciable			1.395	100	(440)	1.389	^{b}	(440)
1.1826	33	(311)				1.140	20	(444)	Not appreciable		
1.1325	12	(222)				1.027	10	(731)			
0.9808	6	(400)				0.989	10	(800)			
0.9000	32	(331)	0.9081	^{a}	(331)	0.884	10	(840)	0.883	^{a}	(840)
0.8773	20	(420)	0.8717	^{a}	(420)	0.804	20	(844)	Not appreciable		

[a] Weak.

[b] Broad.

diffraction observations of catalyst A surface carried out before aging, while Table 3, the ones after aging. In Table 2, the experimental data of crystal lattice spacings are listed together with the corresponding values cited from ASTM Cards for platinum and gamma alumina. Figure 7 is a typical example showing how the diffraction rings have been observed using copper (a) and chromium radiation (b). The patterns are considerably broad due to the fineness of platinum dispersion and lower crystallinity of the transition alumina. It is interesting to note that (331) and (420) planes for platinum and (440) and (840) planes for gamma alumina are observable in the initial catalyst A surface.

In order to check whether a given diffraction line belongs to platinum or alumina of the two-component system, the incident X-ray microbeam can be moved another 100 μm deep to a position where a platinum layer no longer exists. If this ring disappears by doing so, it can be unequivocally attributed to platinum; and if it does not disappear on the contrary, it will belong to alumina. For example, with regard to the outermost line corresponding to γ-Al_2O_3 (440) or Pt (220) spacing, it was found that the ring was retained by this procedure, indicating that the source of this ring was apparently alumina. This procedure was tentatively termed as a "background" technique.

TABLE 3

Microfocused X-Ray Diffraction Reflection from Cross-Sectioned Surface Zone of Catalyst A After Engine Dynamometer Aging

100-hr aging						200-hr aging					
Platinum			Gamma alumina			Platinum			Gamma alumina		
d (Å)	I/I_0	hkl	d (Å)	I/I_0	hkl	d (Å)	I/I_0	hkl	d (Å)	I/I_0	hkl
	NA^a		1.389	^{d}	(440)		NA		1.394	$^{c\ d}$	(440)
0.9015	$^{b\ c}$	(331)		NA			NA			NA	
	NA		0.883	^{d}	(840)	0.877	$^{c\ d}$	(420)		NA	

[a] Not appreciable.

[b] Sharp.

[c] Weak.

[d] Broad.

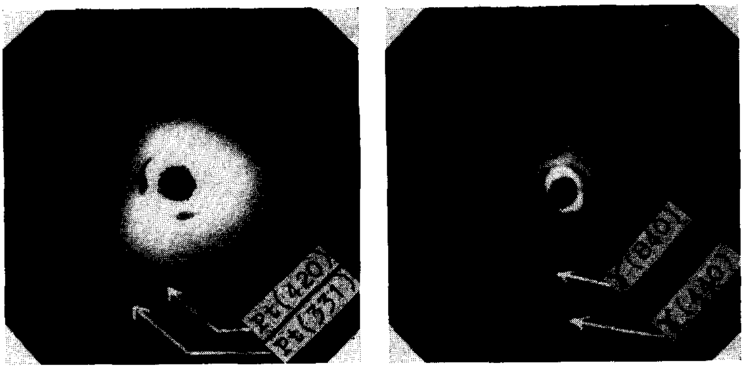

FIG. 7. Typical example of microfocused X-ray diffraction reflection rings from the thin section of the surface zone of catalyst A, obtained with (a) copper radiation and with (b), chromium radiation, respectively.

In Table 4 is shown that catalyst B exhibited no definite diffraction ring of platinum and emerged with a very weak ring of alumina corresponding to (440) for the initial state of surface zone. A broad and indefinite (420) plane of platinum began to appear at 100 hr as seen in Table 5 and this phase settled to be present during another 100 hr. As for alumina, a weak (440) ring was present before aging and this was retained after 200-hr service, while a broad (840) pattern temporarily appeared at 100 hr and this phase was not observed at 200 hr. Repetition of the ASTM data is omitted in Tables 4 and 5.

There were some differences of opinion in the past regarding platinum if it crystallizes or it forms aggregates on the surface of the support (*11*). Figure 8 is the conventional powder X-ray diffraction charts obtained with disintegrated samples of catalysts A and B, before and after aging, which gives only the pattern of transition alumina providing no information regarding platinum because of its minor amount.

However, from the observations of Tables 2–5, it is indicated that there can be both types of platinum phase present for the active surface; a rather crystalline character like catalyst A on one hand, and rather amorphous nature like catalyst B, on the other. Even with the former type of catalyst, it is apparent that platinum in active adherent form on alumina supports will not possess a well developed crystallinity like one seen in the usual form of the metal. For instance, the absence of (311) and (222) lines in catalyst A, which intensities should normally be comparable to (331) or (420) planes according to the ASTM data, is particularly interesting (Table 2). In this connection, the activity data in Figs. 5 and 6 may suggest that specific combination of crystalline phases of platinum and transition alumina, i.e., (331) and (420) planes of platinum with (440) and (840) planes of alumina furnished by catalyst A (Table 2), will be preferred for initial catalytic activity to another type of combination such as amorphous platinum plus (440) plane of alumina in catalyst B (Table 4). It is interesting to note that in the surface zone of both catalysts A and B, the phases present after ultimate 200-hr service have become a similar pattern, bringing about (420) for platinum and (440) for gamma

TABLE 4
MICROFOCUSED X-RAY DIFFRACTION REFLECTION FROM CROSS-SECTIONED SURFACE ZONE OF CATALYST B BEFORE ENGINE DYNAMOMETER AGING

Platinum			Gamma alumina		
d (Å)	I/I_0	hkl	d (Å)	I/I_0	hkl
	NA[a]		1.387		(440)
	NA			NA[b]	
	NA			NA	

[a] Not appreciable.
[b] Very weak.

TABLE 5

MICROFOCUSED X-RAY DIFFRACTION REFLECTION FROM CROSS-SECTIONED SURFACE ZONE OF CATALYST B AFTER ENGINE DYNAMOMETER AGING

100-hr aging						200-hr aging					
Platinum			Gamma alumina			Platinum			Gamma alumina		
d (Å)	I/I_0	hkl	d (Å)	I/I_0	hkl	d (Å)	I/I_0	hkl	d (Å)	I/I_0	hkl
	NA[a]		1.388	[b]	(440)		NA		1.388	[b] [d]	(440)
	NA			NA			NA			NA	
0.8550	[b]	(420)	0.883	[b]	(840)	0.8790	[c]	(420)		NA	

[a] Not appreciable.
[b] Broad.
[c] Sharp.
[d] Weak.

alumina, under the particular aging condition employed (Tables 3 and 5).

As for the innermost line having the *d* value around 0.88 Å, however, it is uncertain whether this is attributed to (840) of a transition alumina modification or to the platinum phases having 0.85–0.88 Å, or to both. This ring was faintly maintained after the "background" technique. The conventional powder X-ray diffraction charts in Fig. 8 provide no information about this particular problem as to what microstructural phase changes took place on the surface. In Fig. 8 no diffraction peaks exist at a higher diffraction angle of 122–124° of 2θ (Cu$K\alpha$) that corresponds to these

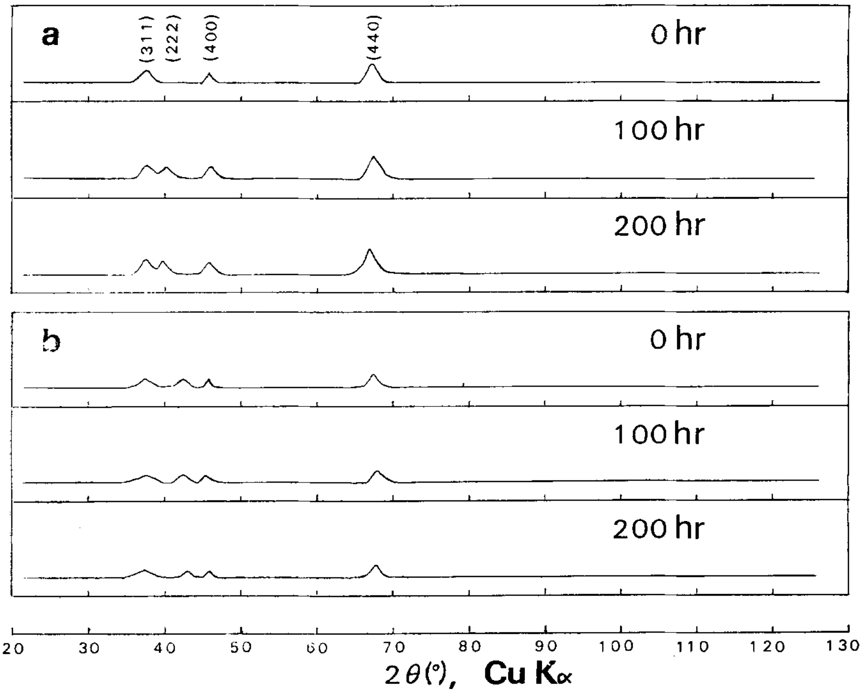

FIG. 8. Typical diffraction patterns obtained by the conventional powder X-ray method, using disintegrated Pt–Al_2O_3 catalyst tablets before and after aging. (a), Catalyst A; and (b), catalyst B.

rings, at any stage of aging. It follows, therefore, that the occurrence of the alteration in phases observed before and after the deactivation process did not take place on the entire tablet body basis, but has been locally produced in the surface zone.

Being different from the characteristics of internal bulk, the unusual behavior of the surface crystallinity observed here offers some analogy with the case of disordered nature of the surface compositions exhibited by some alloy catalysts such as Cu–Ni, Cu–Pd, and Au–Pd for hydrogenation reactions (*12*). It is implied, based on the above experimental observations, that the platinum-dispersed alumina layer on the alumina support may constitute an independent "alloyed" zone of platinum and alumina, though in not strictly a metallurgical sense, but in a sense that it possesses a disordered crystalline arrangement distinguishable from the usual form of platinum as well as from the internal alumina substrate. This alloyed thin area will play an important role on manifestation of the catalyst activity. However, under present geometric condition employed for film installation, the scope of observable X-ray diffraction reflection from the specimen is rather limited to allow a significant extension of discussion on crystal orientation of the active surface.

However, it has been shown that deactivation is closely associated with alteration in crystalline orientation of the thin zone of the catalyst surface. The platinum-dispersed alumina layer of only 100–200 μm deep or so is no doubt an essential part of the entire body of a catalyst tablet. Deactivation phenomena, from the physical point of view, could be attributed to redistribution of the phases present in the active thin zone declining to a stabilized orientation of the constituents with time in use.

ACKNOWLEDGMENTS

The author wishes to thank Mr. H. Yamaguchi and Y. Sakakibara for their cooperation in the microfocused X-ray diffraction measurements which brought this work into being. Thanks are also due to Mr. T. Kobayashi and Mr. M. Yamamoto who made the electron probe microanalysis.

REFERENCES

1. TARAMA, M., "Hanno Betsu Jitsuyo Shokubai (Catalysts Handbook)," p. 90. Kagaku Kogyo Sha, Tokyo, 1970.
2. ALLEN, R. R., AND GERHOLD, C. G., Preprint of The 5th Technical Meeting, Air Pollution Control Association, West Coast Division, San Francisco, 1970.
3. ROTH, J. F., *Ind. Eng. Chem. Prod. Res. Develop.* **10,** 381 (1971).
4. MIYAZAKI, K., Preprint No. 721, Society of Automotive Engineers of Japan, p. 85. 1972.
5. CANNON, W. A., AND WELLING, C. E., *Ind. Eng. Chem. Prod. Res. Develop.* **1,** 152 (1962).
6. HASHIMOTO, H., OZAKI, S., AND OKAWA, T., *Nihon Kessho Gakukai Shi* **8,** 34 (1966).
7. RIGAKU DENKI NEWS PRODUCT, p. 31. 1970.
8. BADDOUR, R. F., MODELL, M., AND GOLDSMITH, R. L., *J. Phys. Chem.* **74,** 1787 (1970).
9. KHASSAN, S. A., EMEL'YANOVA, G. L., LEBEDEV, V. P., AND KOBOZEV, N. I., *Zh. Fiz. Khim.* **44,** 1469 (1970).
10. TAKAHASHI, T., AND TSUNETANI, A., *Kogai* **2,** 18 (1967).
11. ZAIDMAN, N. M., DZIS'KO, V. A., KARNAUKHOV, N. P., KOROEEVA, N. G., AND VISHNYAKOVA, G. P., *Kinet. Katal.* **9,** 863 (1968).
12. CADENHEAD, D. A., AND NASSE, N. G., *J. Phys. Chem.* **70,** 3558 (1966).